ACS OMEGA

http://pubs.acs.org/journal/acsodf

Article

Breathing Mode's Temperature Coefficient Estimation and Interlayer Phonon Scattering Model of Few-Layer Phosphorene

Jeevesh Kumar, Utpreksh Patbhaje, and Mayank Shrivastava*

Cite This: *ACS Omega* 2022, 7, 43462−43467

Read Online

ACCESS | Metrics & More | Article Recommendations | Supporting Information

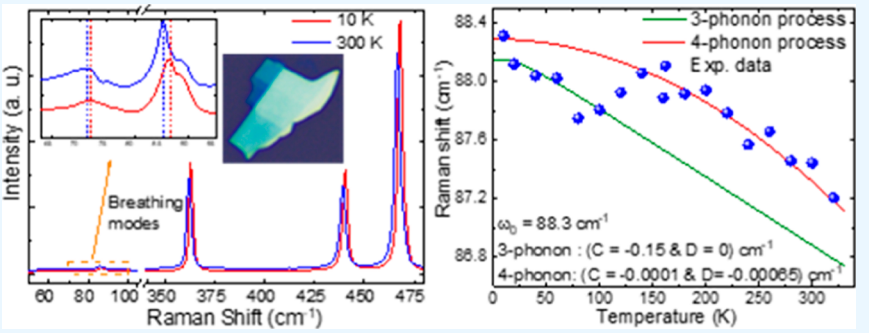

ABSTRACT: The breathing mode's Raman characteristic is a key parameter that estimates the number of layers and helps to determine interlayer thermal coupling in multilayer phosphorene. However, its temperature coefficient is not investigated yet, probably due to phosphorene's ambient instability, difficulties in capturing its Raman modes, and relatively weak temperature sensitivity than the corresponding primary intralayer Raman modes. Here, we captured the breathing modes' Raman scattering in multiple phosphorene flakes at different temperatures and estimated the corresponding first-order temperature coefficient. The captured modes show a negative temperature coefficient of around −0.0025 cm^{-1}/K. Besides, we have explored a unique feature of the breathing mode phonon scattering with temperature. The modes closely follow the dominant three-phonon process and four-phonon process scattering phenomena at low- and high-temperature ranges. The three-phonon process scattering is dominant below ∼100 K, shifting to the dominant four-phonon process scattering beyond ∼150 K. Moreover, the phonon modes show anomalous behavior of blue shift with temperature during 100−150 K, probably due to transition in the scattering process. Our study shows the significant dependency of the breathing modes over temperature, which helps to understand and model phosphorene's interlayer thermal and mechanical properties. The study also reflects that phosphorene has significant interlayer heat transport capability due to three- and four-phonon scattering features.

INTRODUCTION

Phosphorene, a few layers (ideally monolayer) of black phosphorous, consists of various remarkable properties, which make the material a promising candidate for next-generation electronic devices.[1−3] However, many material features are unexplored yet, probably due to its ambient instability.[4,5] Identifying a thin flake of phosphorene is a real challenge for material exploration and device processing due to the risk of degradation during thickness measurement using tools such as AFM.[6] Low-frequency Raman active interlayer phonon modes, known as breathing modes, can provide a promising non-destructive technique to determine thin flakes from the exfoliated 2D materials' flake islands.[7−10] The phonon mode corresponds to interlayer out-of-the-plane vibration in a few layers of black phosphorous. Besides, the breathing mode's properties and thermal evolution can help understand interlayer forces and their thermal coupling in phosphorene, as high-frequency Raman modes talk about the intralayer phonon transport properties of the 2D materials.[11,12]

Despite these features, the breathing mode's thermal evolution and scattering phenomena are not explored extensively yet. Ling et al.[9] found that the breathing mode does not have a significant dependency on temperature, even though the material has promising interlayer coupling.[13,14] Their observations, however, were done over PMMA-coated phosphorene, which may not give precise results due to perturbation in the out-of-the-plane interlayer vibrations. Thus, an extensive probing of the breathing mode is required over unmask phosphorene to fetch the precise value of the breathing mode's Raman positions at different temperatures.

Received: June 16, 2022
Accepted: November 7, 2022
Published: November 21, 2022

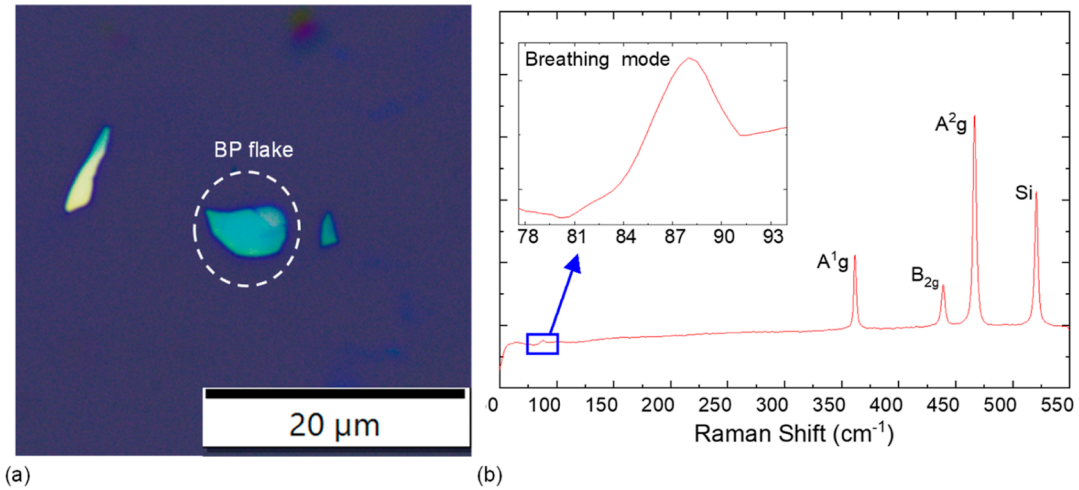

Figure 1. (a) Optical image of a few layers of phosphorene flake captured using an OLYMPUS BX53M microscope with 100× objective. (b) Raman characteristics of the flake, which has three high-frequency modes (A^1g, B_{2g}, and A^2g) and a low-frequency breathing mode (inset).

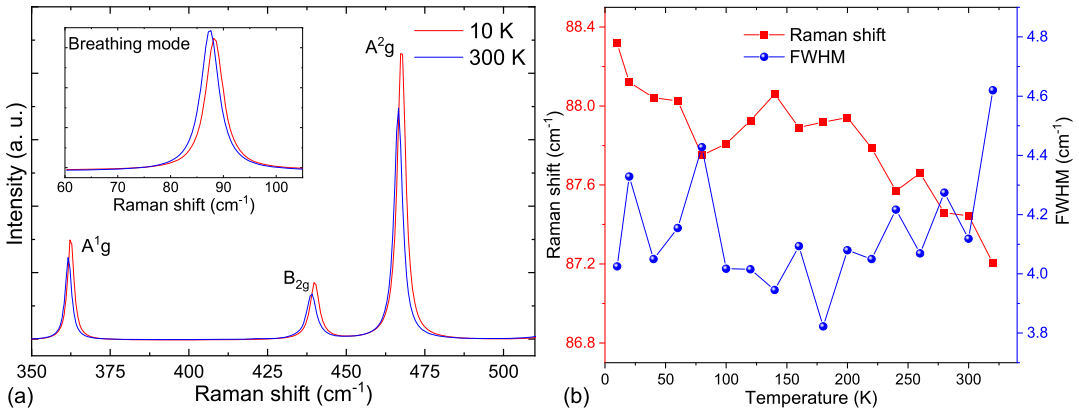

Figure 2. (a) HF and LF (inset) Raman modes of the phosphorene flake (Figure 1a) at 10 and 300 K. HF Raman shifts with different temperatures are given in the Supporting Information (SI, Figure S1). (b) Raman shifts and fwhm of low-frequency breathing modes at different temperatures.

Here, we captured the Raman breathing mode of a few layers of phosphorene flakes from 10 to 320 K to investigate their thermal evolution properties, thereby estimating the first-order temperature coefficient of the breathing mode. Moreover, the Raman shift of the breathing mode with temperature is modeled on the three-phonon process and the four-phonon process scattering. The manuscript starts with a discussion about the thermal evolution of the breathing mode over a few layers of phosphorene flake, followed by estimates of the thermal coefficient of the flake. After that, it explains the three-phonon processes and four-phonon process scattering of the breathing mode. Finally, the manuscript contains thermal evolution and phonon scattering model validation over multiple phosphorene flakes.

RESULTS AND DISCUSSION

After exfoliation, we identified an isolated few layers of phosphorene flake (Figure 1) based on optical contrast and confirmed the black phosphorous material by the presence of the three high-frequency modes (A^1g, B_{2g}, and A^2g) in the Raman characteristics.[15,16] Besides high-frequency Raman modes, which are due to intralayer phonon vibrations, phosphorene also has low-frequency Raman active modes due to interlayer out-of-the-plane vibration, known as the breathing mode.[9,17] We captured the breathing mode (Figure 1b, inset) to examine its thermal evolution and modeling further.

Thermal Evolution of the Breathing Mode. The flake's Raman characteristics were captured at different temperatures. With a temperature rise from 10 to 300 K, the three high-frequency Raman lines (Figure 2a), A^1g, B_{2g}, and A^2g, show a red shift of 0.74, 1.00, and 1.02 cm^{-1}, respectively. The observed red shift behaviors are consistent with previous work,[9] which shows the validity of our experimental setups and processes. The low-frequency breathing mode shows a similar red shift trend with a rise in temperature (Figure 2a, inset). The mode shifts 0.87 cm^{-1} with an increase in temperature from 10 to 300 K. The observed breathing mode (LF) shift is close to the corresponding intralayer high-frequency (HF) modes. Thus, it is worth investigating and estimating its thermal evolution to understand interlayer coupling properties.

The captured breathing mode Raman shift at different temperatures (Figure 2b) shows falling trends (red shift) with temperature rise. The falling curve is shallow at a lower-temperature range and becomes steeper at a higher temperature. The corresponding full width at half-maximum (fwhm) is almost constant at a lower temperature. However, it shows a rising trend at higher temperatures, probably due to more thermal scattering, as observed in the high-frequency Raman modes.[11,14] The significant thermal shift in the breathing

https://doi.org/10.1021/acsomega.2c03759
ACS Omega 2022, 7, 43462−43467

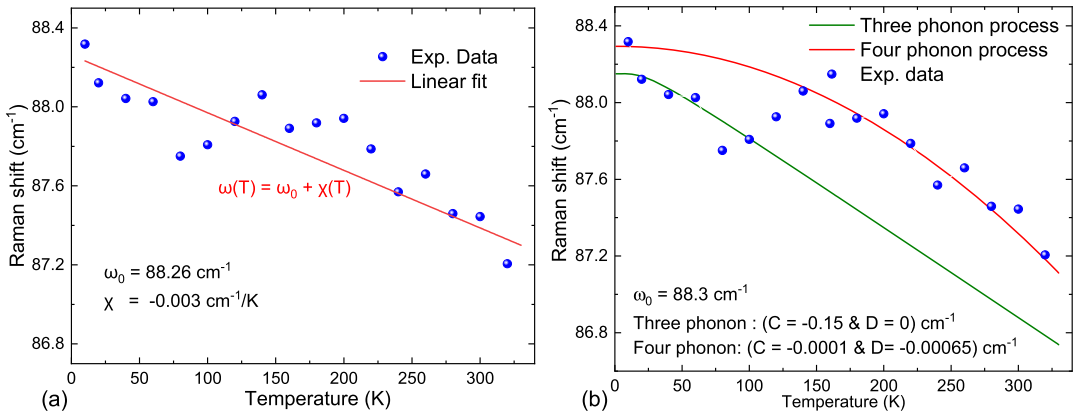

Figure 3. (a) Linear fitting of the temperature-dependent breathing mode's Raman data of the phosphorene flake shown in Figure 1a. (b) Three-phonon and four-phonon process fitting of the Raman data.

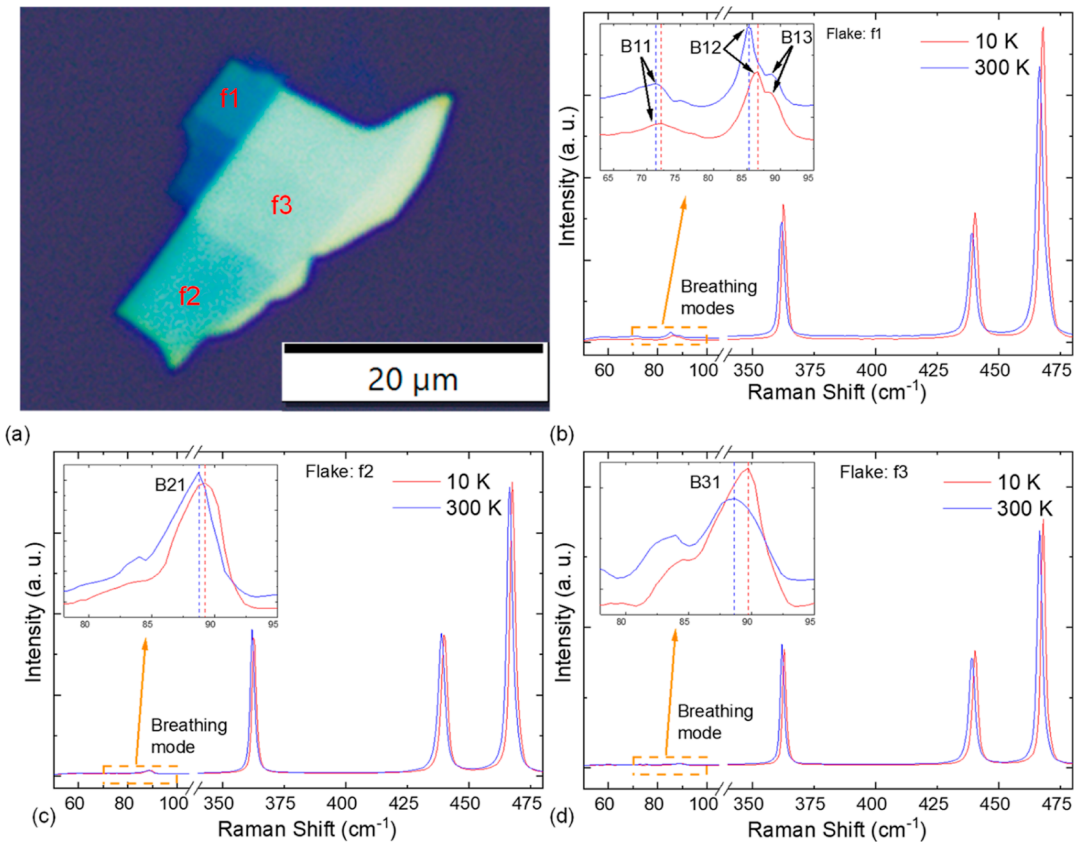

Figure 4. (a) Phosphorene flake has different thickness regions (f1, f2, and f3), captured using an OLYMPUS BX53M microscope with 100× objective. (b–d) Raman spectra of the regions f1, f2, and f3, respectively, at 10 and 300 K. Breathing modes of all the flakes are named in the insets.

modes reflects a relatively strong interlayer anharmonic interaction in the material. Thus, we can say that phosphorene has a significant interlayer interaction for playing an essential role in interlayer thermal transport.

Temperature Coefficient Estimation and Phonon Scattering Model. Usually, the temperature-dependent Raman shift is analyzed and approximated by a first-order linear equation.[9,11,12,14,18,19]

$$\omega(T) = \omega_0 + \chi T \quad (1)$$

where χ is the first-order temperature coefficient and ω_0 is the extrapolated value of the linear fit at zero Kelvin. After fitting with experimental data (Figure 3a), the values of χ and ω_0 are -0.003 cm^{-1}/K and 88.26 cm^{-1} respectively. The approximated temperature coefficient value (-0.003 cm^{-1}/K) is 1 order less than the reported thermal coefficient of HF phonon modes.[9,11,14]

A closer look at the linear fitting reflects that the experimental data significantly deviates from the linear fitted line. Moreover, the data reflect three different regions of the Raman shift behavior. It shows a red shift until 100 K, a blue shift from 100 to 150 K, and a red shift after 150 K. Thus, a much better approximation is needed to explain the thermal evolution of the breathing mode.

Balkanski et al.[20] developed an approach based on the phenomenon of optical phonon decay into two (three-phonon

https://doi.org/10.1021/acsomega.2c03759
ACS Omega 2022, 7, 43462−43467

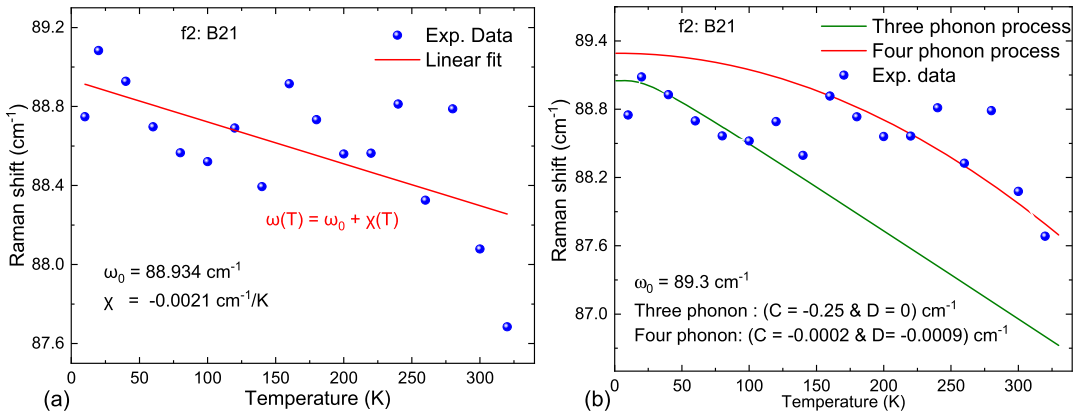

Figure 5. (a) Linear fitting of the temperature-dependent breathing mode's (B21) Raman data of the phosphorene flake "f2" shown in Figure 4a. (b) Three-phonon and four-phonon process fitting of the Raman data.

processes) or three (four-phonon processes) acoustic phonons with equal energies. Based on their model, the temperature-dependent Raman mode positions can be described by the equation

$$\omega(T) = \omega_0 + C\left(1 + \frac{2}{e^x - 1}\right) + D\left(1 + \frac{3}{e^y - 1} + \frac{3}{(e^y - 1)^2}\right) \quad (2)$$

where C and D are anharmonic constants (fitting parameters), ω_0 is the phonon frequency at zero Kelvin, $x = \hbar\omega_0/2kT$, $y = \hbar\omega_0/3kT$, $\hbar$ is the Planck constant divided by 2π, k is the Boltzmann constant, and T is the temperature. The values of C and D are the strength of three-phonon and four-phonon processes, respectively. After fitting, C and D determine the dominant phonon scattering modes in the system. $C/D > 1$ says that the three-phonon process is the dominant scattering mode and vice versa. Tristant et al.[21] and Łapińska et al.[22] explored that the thermal evolution of the HF frequency phonon modes of the few-layer phosphorene has a better explanation using three- and four-phonon scattering model (eq 2) than the first-order linear equation model (eq 1). Thus, it is worth investigating the three- and four-phonon processes scattering the possibility of the breathing mode.

Our experimental data fit on different C and D values for low-temperature (10−∼100 K) and high-temperature (∼150−320 K) ranges (Figure 3b). For low temperature, the fitting parameters are, $\omega_0 \approx 88.3$ cm^{-1}, $C \approx -0.15$ cm^{-1}, and $D \approx 0$. Thus, the modeled equation is

$$\omega(T) = \left[88.33 - 0.15\left(1 + \frac{2}{e^{63.5676/T} - 1}\right)\right] \text{cm}^{-1} \quad (3)$$

For high temperature, the fitting parameters are $\omega_0 \approx 88.3$ cm^{-1}, $C \approx -0.0001$ cm^{-1}, and $D \approx -0.00065$ cm^{-1}. Thus, the modeled equation is

$$\omega(T) = \left[88.33 - 0.0001\left(1 + \frac{2}{e^{63.5676/T} - 1}\right) - 0.00065\left(1 + \frac{3}{e^{42.3784/T} - 1} + \frac{3}{(e^{42.3784/T} - 1)^2}\right)\right] \text{cm}^{-1} \quad (4)$$

The above analysis shows that phosphorene's breathing mode phonon follows three phonon scattering ($C \approx -0.15$ cm^{-1} and $D \approx 0$) until ∼100 K. After that, the scattering process shifts from three-phonon to four-phonon during ∼100 to ∼150 K. Consequently, the four-phonon process ($C \approx -0.0001$ cm^{-1} and $D \approx -0.00065$ cm^{-1}) is the dominant scattering phenomenon in the breathing phonon mode. The blue shift in phonon mode from ∼100 to ∼150 K is probably due to the phonon scattering process transition. The dominance of the four-phonon process is due to more scattering at the higher temperature, as also observed in the rising trend of fwhm (Figure 2b) after ∼150 K.

Validation over Multiple Flakes. We extended our investigation to multiple flakes having different thicknesses for further investigation and validation of temperature-dependent Raman shift. A relatively large flake (Figure 4a) having multiple thickness segments (f1, f2, and f3) was identified based on the contrasts and Raman signatures (Figure 4b−d). The segments f1, f2, and f3 are referred to as flake f1, flake f2, and flake f3, respectively, hereafter. All the flakes show breathing mode characteristics (Figure 4b−d, insets). Moreover, the thinnest flake (f1) has three breathing modes, B11, B12, and B13 (Figure 4b−d, insets), reflecting that a prominent breathing mode is a promising tool for identifying a few-layer phosphorene. All the Raman breathing modes show a significant red shift with temperature. Thus, it validates that the Raman breathing mode position has considerable dependence on temperature.

The prominent isolated breathing mode B21 of flake f2, distinguishable at all temperatures, was captured at different temperatures. Three measurements were done on the flake for all the temperatures, and their average data are plotted in Figure 5. All data plots are given in the Supporting Information (SI, Figure S2). Linear fittings over the averaged data (Figure 5a) show that the first-order temperature coefficient (χ) of the flakes is −0.0021 cm^{-1}/K.

https://doi.org/10.1021/acsomega.2c03759
ACS Omega 2022, 7, 43462−43467

Besides, as discussed in the previous section, the breathing mode follows three-phonon and four-phonon process scattering. The modes follow three-phonon process scattering at the low-temperature range and transform to four-phonon process scattering at the high-temperature range after an anomalous blue shift transition with temperature. Deviation in some experimental data points from the fitting model may be due to experimental artifacts caused by laser heating during multiple measurements, resolution limitation of the detector, and signal deconvolution error. As mentioned in Figure 5b, the fitting parameters (value of C and D) reflect the dominating strength of the three- and four-phonon process scattering at low- and high-temperature ranges, respectively.

Finally, the authors would like to highlight that phosphorene shows a three-phonon to four-phonon scattering shift in the discussed temperature range (around 150−200 K), possibly due to its relatively strong interlayer van der Waal's (vdW) interactions. A similar phonon scattering behavior can be expected at low and high temperatures for the phonons corresponding to very low (like weak vdW) and very high (σ-bond) interactions, respectively. We have captured the breathing mode of another phosphorene flake (few-layer) at different temperatures. The results reflect (SI, Figure S3) different phonon scattering characteristics (three-phonon and four-phonon) at low and high temperatures and possible transitions around ∼150 K. The results are consistent with our manuscript's discussion, further validating our work's authenticity.

CONCLUSIONS

In summary, we captured the breathing modes of multiple few-layer phosphorene flakes and investigated their thermal evolution from 10 to 320 K under high vacuum. All the observed thin flakes reflect prominent breathing modes. The breathing modes show a significant red shift with temperature; therefore, the corresponding linear first-order temperature coefficients (χ) are around −0.0025 cm^{-1}/K. Besides, we explored the phonon scattering model of the breathing modes in the captured temperature ranges. The modes follow three-phonon process scattering at low-temperature ranges. However, the scattering phenomena change to the four-phonon process at a high-temperature range after anomalous blue shift for a short range of temperature rise. Our investigations are consistent with multiple phosphorene flakes, which reflect that phosphorene has considerable interlayer heat transport capability due to three-phonon and four-phonon scattering features.

EXPERIMENTAL DETAILS

Phosphorene was exfoliated over the SiO_2/Si (90 nm) substrate from black phosphorous crystal using the standard blue tape method under a N_2-rich environment. Immediately after exfoliation, the sample was loaded inside the MONTANA helium cryogenic chamber, followed by high vacuum (below 0.1 mTorr) built inside the chamber to protect the flake from ambient degradation. Few-layer phosphorene flakes were identified through the optical window of the chamber based on the contrast and Raman characteristics and validated by capturing the breathing modes. For further investigations, backscattering Raman measurements were done using a HORIBA LabRAM HR with a 532 nm laser source and an OLYMPUS BXFM-ILHS microscope with 50× objective, from 10 to 320 K. Single measurement was done on flake 1 (Figure 1a) for all the temperatures to avoid laser heating that can damage the material. However, for a relatively thicker material (Figure 4a), an average value of the three measurements was taken into account for all the temperatures. We needed high acquisition time (4−10 s, depending on temperature) and accumulation (4−6, depending on the noise level) to capture the breathing modes precisely. During the experiment, the grating number was 1800 gr/mm, and the CCD pixel size was 26 × 26 μm. The signal deconvolution error was around ∼0.01 cm^{-1}.

ASSOCIATED CONTENT

Supporting Information

The Supporting Information is available free of charge at https://pubs.acs.org/doi/10.1021/acsomega.2c03759.

High-frequency Raman shift mode of flake 1; mean and error plot of the prominent breathing mode B21 of flake f2; and three-phonon and four-phonon process fitting of breathing mode Raman data of a few-layer phosphorene flake (PDF)

AUTHOR INFORMATION

Corresponding Author

Mayank Shrivastava − *Department of Electronic Systems Engineering, Indian Institute of Science, Bangalore 560012, India;* orcid.org/0000-0003-1005-040X; Phone: +91 09591140309; Email: mayank@iisc.ac.in

Authors

Jeevesh Kumar − *Department of Electronic Systems Engineering, Indian Institute of Science, Bangalore 560012, India;* orcid.org/0000-0001-6178-8434

Utpreksh Patbhaje − *Department of Electronic Systems Engineering, Indian Institute of Science, Bangalore 560012, India*

Complete contact information is available at: https://pubs.acs.org/10.1021/acsomega.2c03759

Notes

The authors declare no competing financial interest.

ACKNOWLEDGMENTS

The authors would like to thank NNetRA program of MeitY, DST, and MHRD Govt. of India, as well as DRDO and CSIR, for supporting this work.

REFERENCES

(1) Li, L.; Yu, Y.; Ye, G. J.; Ge, Q.; Ou, X.; Wu, H.; Feng, D.; Chen, X. H.; Zhang, Y. Black Phosphorus Field-Effect Transistors. *Nat. Nanotechnol.* **2014**, *9*, 372−377.

(2) Das, S.; Demarteau, M.; Roelofs, A. Ambipolar Phosphorene Field Effect Transistor. *ACS Nano* **2014**, *8*, 11730−11738.

(3) Liu, H.; Du, Y.; Deng, Y.; Ye, P. D. Semiconducting Black Phosphorus: Synthesis, Transport Properties and Electronic Applications. *Chem. Soc. Rev.* **2015**, *44*, 2732−2743 Royal Society of Chemistry May 7.

(4) van Druenen, M. Degradation of Black Phosphorus and Strategies to Enhance Its Ambient Lifetime. *Adv. Mater. Interfac.* **2020**, *7*, 2001102 Wiley-VCH Verlag November 1.

(5) Kumar, J.; Shrivastava, M. First-Principles Molecular Dynamics Insight into the Atomic Level Degradation Pathway of Phosphorene. *ACS Omega* **2022**, *7*, 696−704.

(6) Hyun, C.; Kim, J. H.; Lee, J. Y.; Lee, G. H.; Kim, K. S. Atomic Scale Study of Black Phosphorus Degradation. *RSC Adv.* **2019**, *10*, 350−355.
(7) Jiang, J. W.; Wang, B. S.; Park, H. S. Interlayer Breathing and Shear Modes in Few-Layer Black Phosphorus. *J. Phys.: Condens. Matter* **2016**, *28*, 165401.
(8) Luo, X.; Lu, X.; Koon, G. K. W.; Castro Neto, A. H.; Özyilmaz, B.; Xiong, Q.; Quek, S. Y. Large Frequency Change with Thickness in Interlayer Breathing Mode-Significant Interlayer Interactions in Few Layer Black Phosphorus. *Nano Lett.* **2015**, *15*, 3931−3938.
(9) Ling, X.; Liang, L.; Huang, S.; Puretzky, A. A.; Geohegan, D. B.; Sumpter, B. G.; Kong, J.; Meunier, V.; Dresselhaus, M. S. Low-Frequency Interlayer Breathing Modes in Few-Layer Black Phosphorus. *Nano Lett.* **2015**, *15*, 4080−4088.
(10) Liang, L.; Zhang, J.; Sumpter, B. G.; Tan, Q. H.; Tan, P. H.; Meunier, V. Low-Frequency Shear and Layer-Breathing Modes in Raman Scattering of Two-Dimensional Materials. *ACS Nano* **2017**, *11*, 11777−11802 American Chemical Society December 26.
(11) Su, L.; Zhang, Y. Temperature Coefficients of Phonon Frequencies and Thermal Conductivity in Thin Black Phosphorus Layers. *Appl. Phys. Lett.* **2015**, *107*, 071905.
(12) Yan, R.; Simpson, J. R.; Bertolazzi, S.; Brivio, J.; Watson, M.; Wu, X.; Kis, A.; Luo, T.; Hight Walker, A. R.; Xing, H. G. Thermal Conductivity of Monolayer Molybdenum Disulfide Obtained from Temperature-Dependent Raman Spectroscopy. *ACS Nano* **2014**, *8*, 986−993.
(13) Cai, Y.; Ke, Q.; Zhang, G.; Feng, Y. P.; Shenoy, V. B.; Zhang, Y. W. Giant Phononic Anisotropy and Unusual Anharmonicity of Phosphorene: Interlayer Coupling and Strain Engineering. *Adv. Funct. Mater.* **2015**, *25*, 2230−2236.
(14) Mao, N.; Zhang, S.; Wu, J.; Zhang, J.; Tong, L. Lattice Vibration and Raman Scattering in Anisotropic Black Phosphorus Crystals. *Small Methods* **2018**, *2*, 1700409 John Wiley and Sons Inc June 1.
(15) Feng, Y.; Zhou, J.; Du, Y.; Miao, F.; Duan, C. G.; Wang, B.; Wan, X. Raman Spectra of Few-Layer Phosphorene Studied from First-Principles Calculations. *J. Phys.: Condens. Matter* **2015**, *27*, 185302.
(16) Ribeiro, H. B.; Pimenta, M. A.; de Matos, C. J. S. Raman Spectroscopy in Black Phosphorus. *J. Raman Spectrosc.* **2018**, *49*, 76−90 John Wiley and Sons Ltd January 1.
(17) Mao, N.; Lin, Y.; Bie, Y. Q.; Palacios, T.; Liang, L.; Saito, R.; Ling, X.; Kong, J.; Tisdale, W. A. Resonance-Enhanced Excitation of Interlayer Vibrations in Atomically Thin Black Phosphorus. *Nano Lett.* **2021**, *21*, 4809−4815.
(18) Klemens, P. G. Anharmonic Decay of Optical Phonons. *Phys. Rev.* **1966**, *148*, 845.
(19) Huang, X.; Gao, Y.; Yang, T.; Ren, W.; Cheng, H. M.; Lai, T. Quantitative Analysis of Temperature Dependence of Raman Shift of Monolayer WS2. *Sci. Rep.* **2016**, *6*, 32236.
(20) Balkanski, M.; Wallis, R. F.; Haro, E. Anharmonic Effects in Light Scattering Due to Optical Phonons in Silicon. *Phys. Rev. B: Condens. Matter Mater. Phys.* **1983**, *28*, 1928.
(21) Tristant, D.; Cupo, A.; Ling, X.; Meunier, V. Phonon Anharmonicity in Few-Layer Black Phosphorus. *ACS Nano* **2019**, *13*, 10456−10468.
(22) Łapińska, A.; Taube, A.; Judek, J.; Zdrojek, M. Temperature Evolution of Phonon Properties in Few-Layer Black Phosphorus. *J. Phys. Chem. C* **2016**, *120*, 5265−5270.

https://doi.org/10.1021/acsomega.2c03759
ACS Omega 2022, 7, 43462−43467